Power System Harmonic State Estimation and Observability Analysis via Sparsity Maximization

Huaiwei Liao, *Student Member, IEEE*

***Abstract*— Harmonic state estimation (HSE) is used to locate harmonic sources and estimate harmonic distributions in power transmission networks. When only a limited number of harmonic meters are available, existing HSE methods have limited effectiveness due to observability problems. This paper describes a new system-wide harmonic state estimator that can reliably identify harmonic sources using fewer meters than unknown state variables. Note there are only a small number of simultaneous harmonic sources among the suspicious buses. We propose the concept of S-Observability by extending observability analysis to general underdetermined estimation when considering the sparsity of state variables. We show the underdetermined HSE can become observable with proper measurement arrangements by applying the sparsity of state variables. We formulate the harmonic state estimation as a constrained sparsity maximization problem based on L1-norm minimization. It can be solved efficiently by an equivalent linear programming. Numerical experiments are conducted in the IEEE 14-bus power system to test the proposed method. The underdetermined system contains nine meters and thirteen suspicious buses. The results show that the proposed sparsity maximization approach can reliably identify harmonic sources when presence of measurement noises, model parameter deviations and small non-zero injections.**

***Index Terms*— Power system harmonics, state estimation, wide-area measurements, sparsity, sparsity representation, underdetermined system, observability, waveform distortion, harmonic pollution, meter placement**

I. Introduction

In recent years, the proliferation of power electronic devices and nonlinear loads in power systems has led to increasing concern about the distortion of the sinusoidal waveform of voltage and current in transmission networks due to harmonic pollution. Harmonic pollution is recognized as an important factor in the degradation of power quality, which may shorten equipment life and interfere with communication and control devices [1]. In consequence, the IEEE Harmonic Standard [2] recommends practices for utilities and customers to limit the harmonic contents in power networks. To effectively alleviate harmonic pollution, it is important to identify harmonic sources and estimate the distribution of harmonic voltages and currents by real-time measurements.

The task of harmonic state estimation (HSE)[3],[4] is to locate major harmonic sources and to estimate the distribution of harmonic voltages and currents by partial system-wide measurements. Currently it is feasible to measure the phasors of harmonic voltages and currents in power networks with synchronized measurements. But due to the high expense of harmonic instruments and installation of communication channels, only a limited number of harmonic meters are available in power networks [23] . In other words, the number of measurements are only slightly greater or even fewer than that of unknown state variables. It often results in ill-conditioned or singular measurement matrix in harmonic state estimation, which may cause unreliable estimate when using standard least square (LS) estimator[3].

To overcome the difficulty, a singular value decomposition (SVD) based method[5] is proposed to estimate state variables in observable islands while the rest of the state variables remain unknown. In order to minimize meter requirements as well as to avoid ill-conditioned measurement matrix, optimal meter placement is addressed in [7],[8],[9],[10]. The application of HSE to an actual power system is described in [11], where eight synchronized phasor measurements are used while state variables are seven unknown nodal harmonic current injections. Other approaches, such as artificial neural networks [12], Kalman filters [13],[14],[15], are proposed. In [16],[17], independent component analysis is used to estimate general load injections and harmonic injections.

Despite these efforts, it is still a challenge to estimate reliably all network state variables in even moderate size power networks when provided fewer measurements than suspicious nodes.

An important bit of information about harmonic sources is their spatial sparsity, that is large harmonic injections appear sparsely in the power networks. Alternatively, spatial sparsity means that the simultaneous number of large harmonic sources is much smaller than the number of suspicious buses in practical power systems while their size and location are unknown before state estimation.

By utilizing the sparsity, we show that the underdetermined estimation problem can be solved uniquely via sparsity maximization. This paper is a continuation of our efforts in [18]. The precision of estimates are enhanced by using L_1 norm constraint instead of L_∞ norm in [18]. Some important practical considerations are further investigated.

This paper is organized as follows: Section II gives a description of the problem. In Section III, we describe a new theory for observability analysis in underdetermined systems. Section IV formulates harmonic state estimation as a sparsity maximization problem that can be solved using linear programming tools. Section V addresses meter placement and Section VI gives the results of several numerical experiments using the benchmark IEEE 14-bus harmonic test system.

This work was supported in part by the Alfred P. Sloan Foundation and the Electric Power Research Institute under grants to the Carnegie Mellon Electricity Industry Center, in part by ABB Corporation, and in part by the U.S. National Science Foundation under award CCR-0325892.

H. Liao is with the Department of Electrical and Computer Engineering and Carnegie Mellon Electricity Industry Center, Carnegie Mellon University, Pittsburgh, PA 15213, USA (e-mail: hliao@andrew.cmu.edu).

II. Problem Description

For harmonic analysis in electric transmission systems, we follow the modeling in [19], that is harmonic sources modeled as current sources; transmission equipments as equivalent π-circuits; rotation machines as constant impedance; harmonic filters as shunt impedance; aggregate linear loads as impedance determined by their power in fundamental frequency. The phase shift effect of transformers on harmonic current is also considered. All buses are partitioned into non-source buses, which have neither load injections nor power electronics devices, and suspicious buses, which may have harmonic sources. However, the location of actual harmonic sources is unknown before state estimation. Non-source buses are reduced during the pre-processing stage.

Given harmonic current injections $\dot{\mathbf{I}}(h)$ and harmonic nodal admittance matrix $\mathbf{Y}(h)$, nodal harmonic voltages $\dot{\mathbf{V}}(h)$ can be obtained by solving the harmonic power flow equations as follows:

$$\mathbf{Y}(h)\dot{\mathbf{V}}(h) = \dot{\mathbf{I}}(h) \tag{1}$$

where h stands for the harmonic order. The branch harmonic currents $\dot{\mathbf{I}}_b(h)$ can be obtained subsequently.

Harmonic state estimation is an inverse problem of harmonic power flow. It estimates network state variables with available measurements. Since harmonic source injections can determine all other network variables uniquely, $\dot{\mathbf{I}}(h)$ can be used as state variables.

We choose a subset of nodal voltages $\dot{\mathbf{V}}(h)$ and branch currents $\dot{\mathbf{I}}_b(h)$ as measurements, with all nodal current injections $\dot{\mathbf{I}}(h)$ as state variables. We assume that network topology and parameters in all considered harmonic orders are known. After splitting complex variables into real and imaginary components, the relationship between measurements and state variables can be formulated as follows:

$$\mathbf{z}(h) = \mathbf{H}(h)\mathbf{x}(h) + \mathbf{e}(h) \tag{2}$$

where

$$\mathbf{z} = \begin{bmatrix} \dot{\mathbf{z}}_R \\ \dot{\mathbf{z}}_I \end{bmatrix} \quad \mathbf{x} = \begin{bmatrix} \dot{\mathbf{x}}_R \\ \dot{\mathbf{x}}_I \end{bmatrix} \quad \mathbf{H} = \begin{bmatrix} \tilde{\mathbf{H}}_R & -\tilde{\mathbf{H}}_I \\ \tilde{\mathbf{H}}_I & \tilde{\mathbf{H}}_R \end{bmatrix}$$

h	harmonic order,
m	number of measurements,
n	number of state variables at suspicious buses,
$\mathbf{z}(h)$	$m \times 1$ measurement vector,
$\mathbf{H}(h)$	$m \times n$ measurement matrix,
$\mathbf{x}(h)$	$n \times 1$ state variable vector with excluding nonsource buses,
$\mathbf{e}(h)$	$m \times 1$ measurement error vector.
subscript	$_{R,I}$ denote real and imaginary part respectively

We consider underdeterimed systems in this paper, i.e., $m < n$. Branch current measurements are related to $\mathbf{x}$ by the node-branch distribution factor matrix. Nodal voltage measurements are related to $\mathbf{x}$ by the nodal impedance matrix. Nonsource buses (floating buses) are reduced during pre-processing steps. The measurement errors are assumed as independently and identically distributed (i.i.d.) normal distribution with small variance.

In practical power systems, it is observed that the distribution of harmonic sources has *spatial sparsity*, that is significant harmonic sources appear at only a small fraction of buses simultaneously. Denoting the nodal harmonic current injection vector by $\mathbf{x}$, sparsity means

$$\|\mathbf{x}\|_0 \leq s \tag{3}$$

where $\|\cdot\|_0$ is the L_0 norm, which equals to the number of non-zero entries in the state vector. s gives the maximum number of simultaneous harmonic sources. In this paper, we assume the number of measurements $m > s$ in our analysis.

Considering the spatial sparsity of harmonic sources, we formulate the harmonic state estimation problem as constrained approximated sparsity maximization as follows:

$$\begin{array}{cc} \min\limits_{\mathbf{x}} & \|\mathbf{x}\|_1 \\ \text{subject to} & \|\mathbf{z} - \mathbf{H}\mathbf{x}\|_1 \leq \varepsilon \end{array} \tag{4}$$

where L_1 norm $\|\mathbf{x}\|_1 \triangleq \sum_{k=1}^{n} |x_k|$ is used to approximate L_0 norm, scalar $\varepsilon > 0$ controls the tolerance to residuals. In the following sections we will show that (4) can give an accurate estimate to the underdetermined system (2) under certain conditions.

A standard least-square (LS) estimator is unable to give a reliable estimate for the underdetermined system. As stated in section I, the harmonic state estimator has only a limited number of measurements. It means (2) either has low redundancy ($m = n + k$, k is a small non-negative integer) or is underdetermined ($m < n$). The estimate obtained by the LS estimator,

$$\min_{x} \quad \|\mathbf{z} - \mathbf{H}\mathbf{x}\|_2 \tag{5}$$

is $\hat{\mathbf{x}} = (\mathbf{H}^T\mathbf{H})^{-1}\mathbf{H}^T\mathbf{z}$. For the underdetermined case, the matrix $\mathbf{H}^T\mathbf{H}$ is singular. It leads to unbounded estimation errors. Even in the low-redundancy case, $\mathbf{H}^T\mathbf{H}$ may become close to singular or ill-conditioned. It can cause the failure of LS estimator.

III. Observability Analysis with Sparsity Prior

Observability analysis determines the necessary conditions for the uniqueness of estimates. An observable linear estimator generally requires full column rank of its measurement matrix. In this section, we will show the underdetermined linear system (2) can become observable when state variables are sparse. A closely related topic in signal processing is called optimally sparse representation.

A. Motivation

The linear system $\mathbf{y} = \mathbf{A}\mathbf{x}$ ($\mathbf{y}$ is output) is non-observable if $\mathbf{A}$ does not have full column rank. But if some prior knowledge about $\mathbf{x}$ is available, we may make the system observable. For instance, if we know in advance that only one entry of $\mathbf{x}$ is nonzero,i.e., $\|\mathbf{x}\|_0 = 1$, we can do an n-step test to find the exact solution if none of two columns of $\mathbf{A}$ is linear dependent. Note that we don't know which entry of $\mathbf{x}$ is non-zero in advance. We illustrate this with the following example.

Suppose output $\mathbf{y} = [y_1, y_2]^T$ is generated by the linear equation

$$\left[\begin{array}{c} y_1 \\ y_2 \end{array}\right] = \mathbf{A}_{2\times 3}\mathbf{x}^*_{3\times 1} = [\alpha_1, \alpha_2, \alpha_3]\left[\begin{array}{c} 0 \\ d \\ 0 \end{array}\right]$$

where the internal state variable $\mathbf{x}^*$ is 1-sparse. To obtain $\mathbf{x}^*$ from $\mathbf{y}$, we design a 3-step test. At the k-th step, let

$$\left\{\begin{array}{ll} x_i^{(k)} = x_k & i = k \\ x_i^{(k)} = 0 & i \neq k \end{array}\right.$$

we check the corresponding mismatch vector

$$\begin{aligned} \mathbf{r}^{(k)} &= \mathbf{y} - [\alpha_1, \alpha_2, \alpha_3]\mathbf{x}^{(k)} \\ &= \mathbf{y} - \alpha_k x_k \end{aligned} \tag{6}$$

Obviously, if any two of the column vectors $\alpha_1, \alpha_2, \alpha_3$ are linearly independent, for any x_1, x_2, x_3, we must have

$$\mathbf{y} - \alpha_1 x_1 \neq \mathbf{y} - \alpha_2 x_2 \neq \mathbf{y} - \alpha_3 x_3 \tag{7}$$

Here only $x_2 = d$ can achieve zero mismatch. Thus, the unique solution is given by $\mathbf{x}^{(2)} = [0, d, 0]^T$. Therefore, the underdetermined system is observable if at least two column vectors are linearly independent when $\mathbf{x}$ has only one non-zero entry.

B. Sparsity Prior and Matrix Spark

Definition 1 (Sparsity): Vector $\mathbf{x}$ is *s-sparse* if only s of its entries are nonzero.

Remark 1: x is *s-sparse* $\Leftrightarrow$ $\|\mathbf{x}\|_0 = s$. Note that this definition does not provide any information about the exact location of these non-zero entries.

Sparsity prior therefore is referred to as the prior knowledge about the maximum number of non-zero entries in the unknown vector.

Definition 2 (Spark): [20]The *spark* of matrix $\mathbf{A}$ is defined as the smallest possible number of its columns that are linearly dependent.

Remark 2: Another interpretation of $spark(\mathbf{A})$ for an m-by-n matrix $\mathbf{A}$ is: $spark(\mathbf{A}) = s$, if all of its $m \times (s-1)$ submatrices have full column rank and at least one of its $m \times s$ submatrices is singular. Clearly, for any matrix $\mathbf{A}$ without zero columns, $2 \leq spark(\mathbf{A}) \leq Rank(\mathbf{A}) + 1$.

C. Observability of Underdetermined Systems

Motivated by the example, we can generalize the observation to general underdetermined linear systems

$$\mathbf{y}_{m\times 1} = \mathbf{A}_{m\times n}\mathbf{x}_{n\times 1} \tag{8}$$

where $\mathbf{y} \in \mathbf{C}^m$ denotes measurable output, $\mathbf{x} \in \mathbf{C}^n$ denotes state variables, $\mathbf{A} \in \mathbf{C}^{m\times n}$ is a known matrix, and $m < n$. The conditions for its observability are given by the following theorem:

Definition 3 (Observability): A system is *observable* if its internal state $\mathbf{x}$ can be uniquely determined by its output $\mathbf{y}$.

Definition 4 (S-Observability): A system is *s-observable* if it is observable when its internal state $\mathbf{x}$ is at most s-sparse, i.e. $\|\mathbf{x}\|_0 \leq s$.

Theorem 1 (Conditions on S-Observability): The underdetermined linear system (8) is observable if $\mathbf{x}$ is at most s-sparse and $s < \frac{1}{2}spark(\mathbf{A})$, where matrix $\mathbf{A}$ is known and $m < n$.

Proof: (Proof by Contradiction.) According to the definition of observability, (8) is observable if it has unique solution. Assume we have non-unique s-sparse solutions $\mathbf{c}$ and $\mathbf{d}$, $\mathbf{c} \neq \mathbf{d}$, such that

$$\left\{\begin{array}{l} \mathbf{y} = \mathbf{A}\mathbf{c} = \sum_{i=1}^{s} c_{k_i}\alpha_{k_i} \\ \mathbf{y} = \mathbf{A}\mathbf{d} = \sum_{j=1}^{s} d_{p_j}\alpha_{p_j} \end{array}\right. \tag{9}$$

where $\alpha_{k_i}$is the k_i-th column of $\mathbf{A}$. Easily to see

$$\sum_{i=1}^{s} c_{k_i}\alpha_{k_i} + \sum_{j=1}^{s}(-d_{p_j})\alpha_{p_j} = \mathbf{0} \tag{10}$$

The left side of (10) is a linear combination of at most $2s$ different column vectors. Because $spark(\mathbf{A}) > 2s$, any $2s$ or less than $2s$ column vectors of $\mathbf{A}$ must be linearly independent. Therefore (10) can never be true. The solution of (8) is unique.

An exhaustive search algorithm can find the unique solution. It tests all of possible combinations of s non-zero entries of $\mathbf{x}$. Among all combinations

$$\mathbf{x}^{(k)} = [x_{k_1}, \ldots, x_{k_s}]$$

only the combination corresponding to the unique solution $\mathbf{x}^*$ can satisfy the equation

$$\sum_{i=1}^{s} x_{k_i}\alpha_{k_i} = \mathbf{y} \tag{11}$$

The existence of the correct combination is guaranteed by the uniqueness of the solution. Since the combination number $\binom{n}{s}$ is finite, we always can find the real solution within finite steps. This completes the proof. ■

Theorem 1 indicates that if the state vector $\mathbf{x}^*$ has at most s non-zero entries, then it is possible to use not less than $2s$ independent measurements to estimate $\mathbf{x}^*$ if the corresponding $\mathbf{A}$ satisfies $spark(\mathbf{A}) > 2s$. In other words, it is possible to estimate n sparse variables with m $(2s < m < n)$ measurements with proper measurement arrangements.

IV. State Estimation by Sparsity Maximization

Note that among all solutions to underdetermined system (8) there is only one satisfying $\|\mathbf{x}\|_0 < \frac{1}{2}spark(\mathbf{A})$. Alternatively, the sparsest solution is the unique solution when sparsity prior is applied. This leads to the following corollary:

Corollary 1 (The sparsest solution is unique): With the sparsity prior

$$\|\mathbf{x}\|_0 < \frac{1}{2}spark(\mathbf{A})$$

the sparsest solution for (8) is also the unique solution.

We apply Corollary 1 to harmonic state estimation with the sparsity prior of source distribution. Thus, the HSE problem is to find the sparsest solution $\hat{\mathbf{x}}$ while minimizing the residual $\|\mathbf{z} - \mathbf{H}\hat{\mathbf{x}}\|$. It is formulated as follows:

$$\begin{array}{cc} \min\limits_{\mathbf{x}} & \|\mathbf{x}\|_0 \\ \text{subject to} & \|\mathbf{z} - \mathbf{H}\mathbf{x}\|_1 \leq \varepsilon \end{array} \tag{12}$$

When measurement noises are negligible, (12) becomes a sparse representation problem[20],

$$\min_{\mathbf{x}} \quad \|\mathbf{x}\|_0 \quad \text{subject to} \quad \mathbf{z} = \mathbf{H}\mathbf{x} \tag{13}$$

The observability of the underdetermined state estimator is guaranteed by choosing a proper measurement matrix $\mathbf{H}$ such that

$$spark(\mathbf{H}) > 2s \tag{14}$$

where s is the maximum possible number of simultaneous major harmonic sources in the network. Moreover, we can check the correctness of a solution by testing the sparsity condition: $\|\mathbf{x}\|_0 \leq spark(\mathbf{H})/2$.

However, it is difficult to obtain the global optima of (12) by standard convex programming because the problem (12) has a combinatorial nature. The naive strategy used in the proof of Theorem 1 for locating the harmonic sources is to test all possible combinations of k source locations($k \leq s$) and choose the sparsest one with lower-than-threshold residual. The drawback of the naive strategy is that even when s is a moderate number, it has to test an exponential number of potential combinations, which is $\Sigma_{k=1}^{s}\binom{n}{k}$. For instance, when $s = 5$, $n = 100$, the number is around 7.9×10^7.

To avoid the difficulties involved in the sparsity maximization problem (12), there is a series of efforts(generalized in [21] and [20]) for finding an approximation of (12) by replacing $\|\mathbf{x}\|_0$ with other functions $g(\mathbf{x})$. In particular, $g(\mathbf{x}) = \|\mathbf{x}\|_1$ is favored due to its simplicity. The corresponding constrained L_1 norm minimization problem is

$$\min_{\mathbf{x}} \quad \|\mathbf{x}\|_1 \quad \text{subject to} \quad \mathbf{z} = \mathbf{H}\mathbf{x} \tag{15}$$

The conditions on the equivalence of (13) and (15) are established by the following theorem[20].

Definition 5 (Coherence): Coherence of a matrix $\mathbf{A} = [\alpha_1, \ldots, \alpha_n]$ is defined as the maximum absolute inner product between unitary column vectors

$$\mu(\mathbf{A}) \triangleq \max_{1 \leq i \neq j \leq n} |\langle \alpha_i, \alpha_j \rangle| \tag{16}$$

Theorem 2 (Equivalence of (13) and (15)): If (13) has unique solution $\mathbf{x}^*$ and

$$\|\mathbf{x}^*\|_0 < \frac{1}{2}\left(1 + \frac{1}{\mu(\mathbf{A})}\right) \tag{17}$$

then $\mathbf{x}^*$ is also the unique solution of (15).

Remark 3: A proof of this theorem is provided in [20]. This theorem indicates that we can use L_1 norm minimization (15) to replace L_0 norm minimization (13) if the solution is sparse enough. Note that the sparsity bound condition (17) in Theorem 2 is conservative.

The equivalence of L_0-norm and L_1 norm minimization is illustrated by the 2-variable example shown in Fig. 1. Intuitively, Fig. 1 illustrates that when $0 < p \leq 1$, the family of L_p norm minimization share the same solution. Furthermore, L_0 norm is approximated by L_p norm when $p \rightarrow 0$.

When measurement noise exists, we use (4) to replace (15). Our numerical experiments show that the estimate from (4) is stable under small model and measurement disturbances if the underdetermined estimator is s-observable.

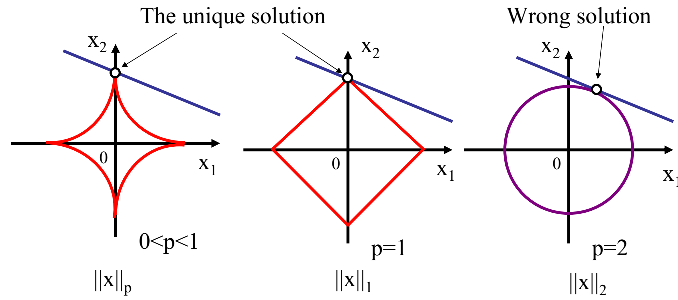

Fig. 1. Illustration that L_1 norm minimization can produce the unique solution given by L_p ($0 < p < 1$) norm minimization problem: $\min_{x_1,x_2} |x_1|^p + |x_2|^p$, $s.t. \phi_1 x_1 + \phi_2 x_2 = c$.

The optimization problem (4) can be cast into a standard linear programming problem (see Appendix for details), which can be solved reliably by simplex methods or interior point methods[22].

V. Meter Placement

From Theorem 1, the spark of measurement matrix $\mathbf{H}$ determines the observability of the underdetermined system. Proper meter placement is needed to make the system observable. Fixing the number of simultaneous harmonic sources L, the meter placement problem is to find the subset of k ($k > 2L$) candidate measurements that make the spark of the corresponding measurement matrix greater than $2L$. Thus:

$$\begin{array}{cc} \min_{\mathbf{y}} & \|\mathbf{y}\|_0 \\ \text{subject to} & spark(\mathbf{H}_c^T \mathbf{y}) \geq 2L \end{array} \tag{18}$$

where $\mathbf{y}$ is $m_c \times 1$ meter selector, $y_i = 1$ indicates that the ith candidate meter is chosen, $y_i = 0$ means meter i is not chosen; $\mathbf{H_c}$ is an $m_c \times n$ complex matrix, which represents the pool of m_c candidate measurements.

Since optimal meter placement is not the primary focus of this paper, we employ a simple greedy search method for meter placement[18]. When the number of meters is fixed, the algorithm is:

1) Determine the maximum number of simultaneous harmonic sources in the network. Denote it as s;
2) Establish the harmonic admittance matrix $\mathbf{Y}(h)$. Set nodal harmonic injection as state variables $\mathbf{x}$;
3) Establish candidate measurement matrix $\mathbf{H}$ and Compute $\mu(\mathbf{H})$;
4) Remove the meters whose removal causes the least increase of $\mu(\mathbf{H})$;
5) Repeat Step 3 and Step 4 until the placed meters are reduced to the pre-set number;
6) Checking the extended observability of $\mathbf{H}$ according to Theorem 1;

7) Repeat Step 1 through Step 6 for each harmonic order;
8) Choose the meter group such that the system is s-observable for each harmonic orders.

We test the proposed meter placement algorithm in the IEEE 14-bus test system shown in Fig. 2. As a result of the placement, a 9-meter group is chosen as shown in Fig 2. The group measures the harmonic currents through line $1-5$, $2-3$,$3-4$, $6-12$, $7-8$, $9-14$, $10-11$, $13-12$ and $13-14$. The calculated spark of the corresponding complex measurement matrix is 10. As a result of Theorem 1, the underdetermined estimator can handle up to $s < 10/2 = 5$ simultaneous complex-valued harmonic sources without the presence of noises.

VI. Numerical Experiments and Discussion

We choose IEEE 14-bus test system[19] to test the proposed method. It is the benchmark system for harmonic study in three-phase balanced transmission networks. We assume all nodes except node 7 (it is a non-source bus) can have harmonic source injections. Thus there are 13 suspicious nodes. For each harmonic order, two harmonic sources are randomly placed in the network. Only 9 meters, shown in Fig. 2, are used by the proposed algorithm. They all take the measurements for branch harmonic currents. The meter placement scheme is the result of the placement algorithm described in Section V.

We use the artificial harmonic injections as "actual" harmonic sources, labeled $\dot{\mathbf{I}}^{(act)}$. "Actual" nodal harmonic voltages $\dot{\mathbf{V}}^{(act)}$ are calculated by the harmonic power flow using the "actual" harmonic injections.

The measurement data are generated by solving the harmonic power flow equation (1) with given harmonic admittance matrices and current injections. Measurement noises are added if necessary. Measurement errors are modeled as i. i. d. (independently and identically distributed) normal distribution with zero mean.

The harmonic state estimation is repeated for each harmonic order to obtain the injection estimate $\dot{\mathbf{I}}^{(est)}$. Then the estimated harmonic nodal voltages $\dot{\mathbf{V}}^{(est)}$ are calculated using harmonic power flow (1) and estimated current injections.

The state estimator only uses the measurements and measurement matrices. Other information such as the location, magnitude and number of harmonic sources are unknown before state estimation is finished. The program is coded using Matlab 7.0 . Simplex method is used to solve linear programming (25), see Appendix.

The root mean square errors (RMS) of voltage magnitude $V_M(\%)$, voltage angle V_A, injection magnitude $I_M(\%)$, and injection angle I_A in each harmonic order are used to compare estimated and simulated values, where the RMS injection errors are averaged by the number of major sources and RMS voltage errors by the total node number.

A. Experiment 1 (noiseless measurements)

In the experiment, we assume the measurement noise is zero. We set the tolerance parameter for equation (4) to 0.001.

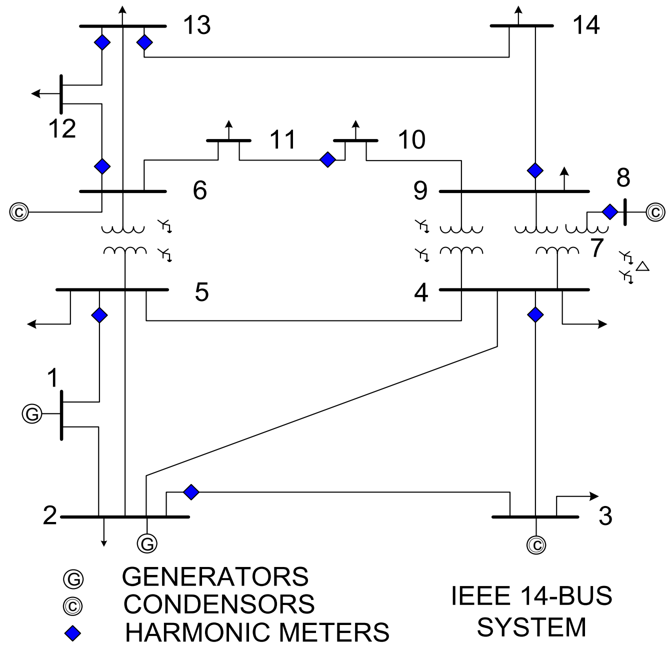

Fig. 2. IEEE 14-bus test system with nine meters

TABLE I

Experiment 1: root mean square errors between estimated and simulated values. $V_M(\%)$, V_A, $I_M(\%)$ and I_A, are the RMS error of voltage magnitude, voltage angle, injection magnitude and injection angle, respectively.

	5th	7th	11th	13th	17th	19th	23rd	25th
$I_M(\%)$	0.18	0.13	0.32	0.19	0.45	1.50	0.11	0.69
$I_A(^\circ)$	0.05	0.06	0.05	0.05	0.06	0.21	0.01	0.19
$V_M(\%)$	0.03	0.01	0.15	0.02	0.04	0.08	0.02	0.19
$V_A(^\circ)$	0.02	0.01	0.03	0.02	0.02	0.11	0.01	0.08

For each harmonic order, harmonic sources can appear at any two buses except the non-source bus 7. The proposed state estimation algorithm (4) is conducted for each harmonic order. The estimated and simulated injection magnitude and voltage magnitude are compared in Fig. 3. The root mean square errors (RMS) of voltage magnitude $V_M(\%)$, voltage angle $V_A(^\circ)$, injection magnitude $I_M(\%)$, and injection angle $I_A(^\circ)$ in each harmonic order are listed in TABLE I. We can see the estimation errors are almost zero for voltages and injections. Moreover both the location and the magnitude of unknown harmonic sources are identified correctly and precisely.

B. Experiment 2 (noisy measurements)

We conduct this experiment to see if the proposed algorithm is stable with presence of measurement noises. We assume the measurement noises obey zero-mean normal distribution with 5% standard deviation and set the tolerance parameter ε as 0.001. All the other settings are the same as that in experiment 1. Two harmonic sources are placed in two randomly selected buses in each harmonic order. The proposed estimation algorithm is performed to obtain injection estimate for each harmonic order. Nodal voltages are calculated using

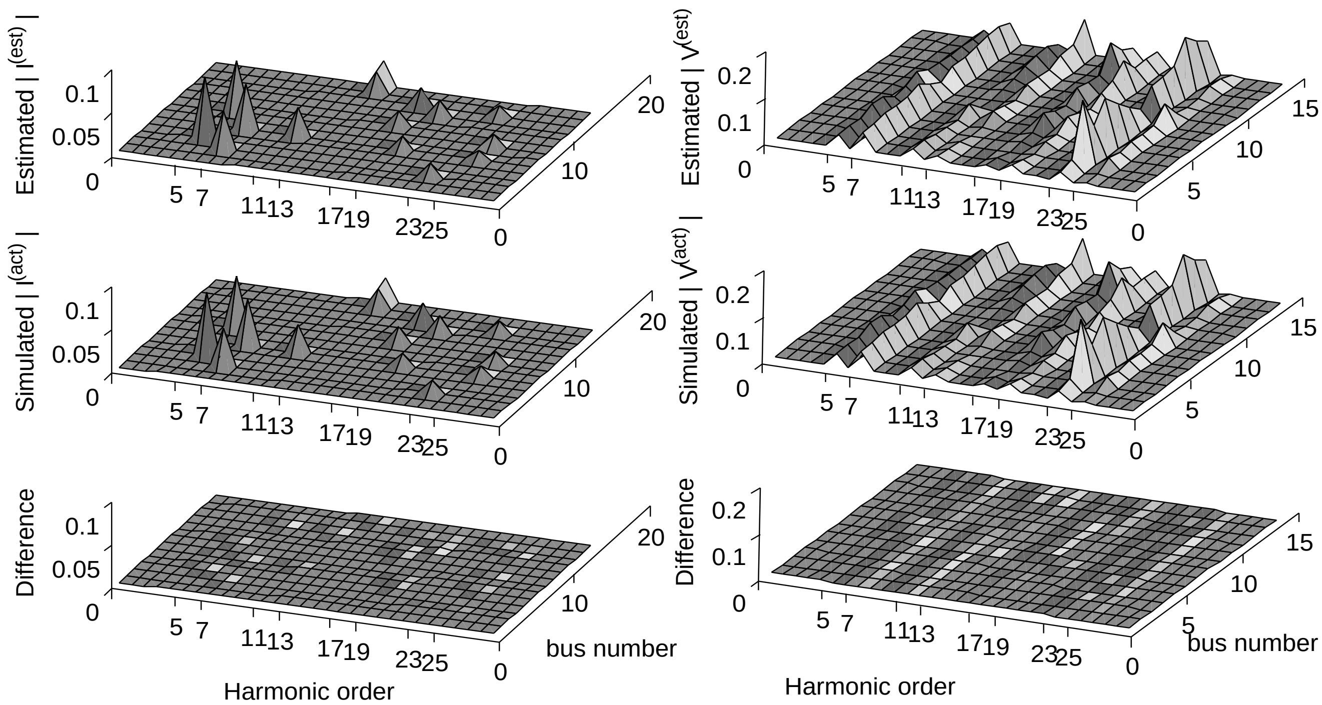

Fig. 3. Results of experiment 1: comparison of estimated and simulated the magnitude of nodal harmonic current injections and voltages in each harmonic order with noiseless measurements and accurate model parameters for IEEE 14-bus test system.

TABLE II

EXPERIMENT 2: ROOT MEAN SQUARE ERRORS BETWEEN ESTIMATED AND SIMULATED VALUES. $V_M(\%)$, $V_A(^\circ)$, $I_M(\%)$ AND $I_A(^\circ)$, ARE THE RMS ERROR OF VOLTAGE MAGNITUDE, VOLTAGE ANGLE, INJECTION MAGNITUDE AND INJECTION ANGLE, RESPECTIVELY.

	5th	7th	11th	13th	17th	19th	23rd	25th
$I_M(\%)$	3.93	1.97	2.27	7.37	4.82	3.29	2.04	5.38
$I_A(^\circ)$	0.32	0.05	0.57	2.74	1.59	1.08	1.15	0.31
$V_M(\%)$	1.17	2.07	0.44	1.86	1.31	0.32	0.89	2.33
$V_A(^\circ)$	0.43	0.51	0.23	0.46	0.67	0.16	0.39	1.42

the estimated injection afterwards. Estimated and simulated the magnitude of nodal harmonic injections and voltages are compared in Fig. 4.

The results show that all harmonic sources in all harmonic orders are identified correctly with small differences from the simulated values. Listed in TABLE II, the RMS errors of voltage magnitude $V_M(\%)$, voltage angle V_A, injection magnitude $I_M(\%)$, and injection angle I_A in each harmonic order are also small.

C. Experiment 3 (Inaccurate model + noisy measurements + small nonzero harmonic sources)

In experiment 1 and 2, we assume the model parameters are accurate. However, in real power systems, the network harmonic parameters can only be obtained in limited precisions. Additionally, we assume that harmonic injections at all other buses are zero except those having major sources. Strictly speaking, it is only partially true because some other buses may have small but non-zero harmonic injections.

This experiment is to test the robustness of the proposed method under less ideal conditions, including the existence of small modeling deviations, noisy measurements and small non-zero sources.

We construct $\hat{\mathbf{H}}$ by disturbing each element of $\mathbf{H}$ by adding i.i.d Gaussian noises with zero mean and 5% standard deviation. $\hat{\mathbf{H}}$ is used in (4) to obtain estimates. The true $\mathbf{H}$ is used to generate “actual” harmonic voltages and currents. “Actual” harmonic injections consisting of 2 major injections and 11 small injections are randomly placed at 13 buses with one injection at one bus. Note that the locations of major harmonic injections are different for each harmonic order. The magnitudes of the 11 small injections are generated by zero-mean normal distribution with 5% standard deviation relative to the largest injection. Their angles are randomly chosen from 0° to 360° . Other settings are the same as those in experiment 2. The measurement noises in Experiment 3 are generated in the same way as those in Experiment 2.

Fig. 5 shows the comparison of estimated and simulated harmonic injection and voltage magnitudes. The RMS errors of $V_M(\%)$,$V_A(^\circ)$, $I_M(\%)$, and $I_A(^\circ)$ in each harmonic order are listed in TABLE III. The results show that all major harmonic sources in all harmonic order are located correctly though there are 12.58% and 16.23% injection magnitude errors in 13rd and 23rd harmonics.

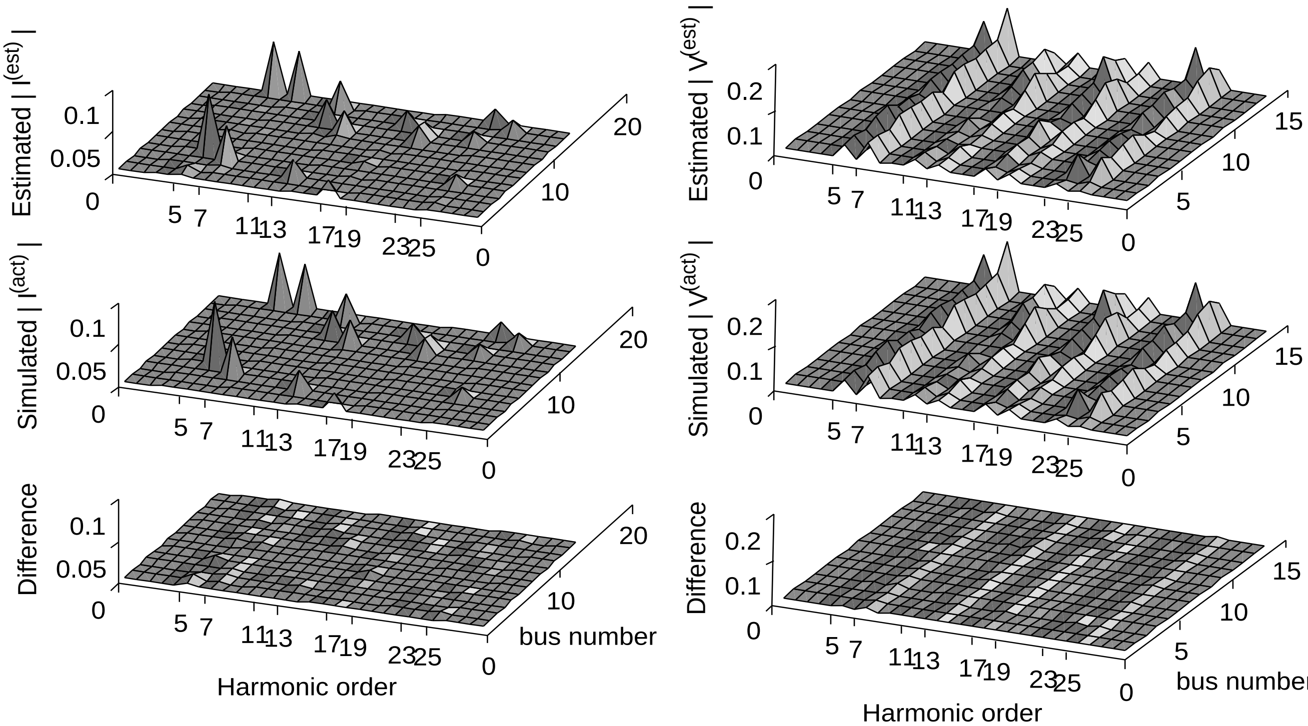

Fig. 4. Results of experiment 2: comparison of estimated and simulated the magnitude of nodal harmonic injections and voltages in each harmonic order for IEEE 14-bus test system when measurement noises obey zero-mean normal distribution with 5% standard deviation.

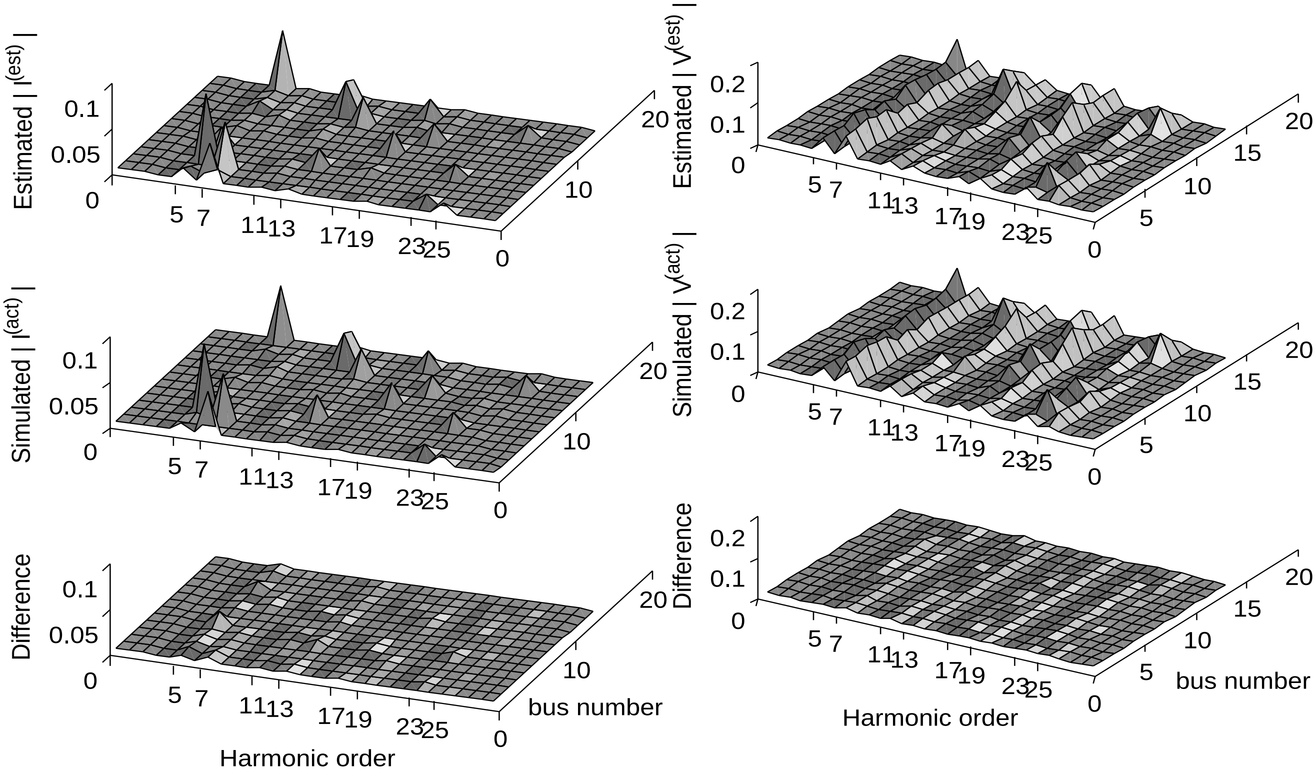

Fig. 5. Results of experiment 3: comparison of estimated and simulated nodal harmonic voltage magnitudes and current injections in each harmonic order for IEEE 14-bus test system with small modeling deviation, two large sources, 11 small non-zero sources and noisy measurements.

TABLE III

EXPERIMENT 3: ROOT MEAN SQUARE ERRORS BETWEEN ESTIMATED AND SIMULATED VALUES. $V_M(\%)$, V_A, $I_M(\%)$ AND I_A, ARE THE RMS ERROR OF VOLTAGE MAGNITUDE, VOLTAGE ANGLE, INJECTION MAGNITUDE AND INJECTION ANGLE, RESPECTIVELY.

	5th	7th	11th	13th	17th	19th	23rd	25th
$I_M(\%)$	3.40	4.82	0.61	12.6	0.65	4.41	16.2	4.25
$I_A(°)$	1.71	2.33	0.86	0.71	1.39	0.28	2.34	2.22
$V_M(\%)$	3.06	1.85	20.6	6.24	5.89	1.98	4.08	2.71
$V_A(°)$	1.89	0.54	13.0	5.52	15.4	0.53	2.14	5.67

D. Discussion

The numerical experiments show that the proposed underdetermined estimator is capable of identifying the harmonic sources reliably when considering noisy measurements and small model parameter errors. Moreover the calculated nodal voltage phasors using estimated injections are very close to the simulated values. Thus all state variables of the network are obtained with satisfactory precisions. Since Theorem 1 is also valid for overdetermined systems, our numerical results (not listed here) show that the proposed algorithm is able to obtain accurate estimate for ill-conditioned overdetermined systems while least square estimator fails and SVD estimator obtains a reliable estimate only for partial networks.

If replacing the L_1 norm in the constraint in (4) by L_2 norm, we have a new estimator:

$$\begin{array}{cc} \min\limits_{\mathbf{x}} & \|\mathbf{x}\|_1 \\ \text{subject to} & \|\mathbf{z}-\mathbf{H}\mathbf{x}\|_2 \leq \tau^2 \end{array} \tag{19}$$

where scalar $\tau > 0$ controls the tolerance to residuals. Another variant[18] of (4) can be obtained if we use the Infinity norm L_∞ to replace L_1.

$$\begin{array}{cc} \min\limits_{\mathbf{x}} & \|\mathbf{x}\|_1 \\ \text{subject to} & \|\mathbf{z}-\mathbf{H}\mathbf{x}\|_\infty \leq \eta \end{array} \tag{20}$$

where scalar $\eta > 0$ controls the tolerance to residuals. Our simulation results show that (19)>(4)>(20) in terms of the accuracy of estimate while all of the three locate harmonic sources correctly.

We prefer (4) to (19) because the main task for HSE is to identify harmonic sources reliably and both (4) and (19) have the same capability for achieving that task. But (4) can be solved efficiently and reliably by linear programming while to solve (19) needs general convex programming. Moreover, we choose (4) instead (20) because (4) gives more accurate estimate while both of them can be solved effectively in linear programming.

To enhance the estimate accuracy, an additional least square estimator can be conducted after identifying the location of harmonic sources.

Although we use three-phase balanced power network models in proposed algorithm and numerical experiments, there is no fundamental difficulty to extend the proposed method to three-phase unbalanced systems. In unbalanced systems, both the measurements and the state variables become three-phase quantities. And the measurement matrix can be made according to the three-phase parameters and topology of the unbalanced network.

Further work will focus on the following issues:

1) Fast analysis of S-observability and optimal meter placement;
2) Efficient implementation of the proposed method in real large-scale power networks;
3) Harmonic state estimation considering three-phase unbalanced power network models;
4) Reduction of the effect of gross errors and modeling errors on estimate.

VII. CONCLUSION

This paper proposes a systematic approach to identify and estimate harmonic sources in power networks when the number of harmonic meters is less than the number of unknown state variables. In such an underdetermined system, full observability cannot be ensured via traditional observability approaches. It leads to the failure of existing least square based methods. To resolve the observability problem, we construct the proposed state estimator by considering nodal harmonic injections as state variables. Then, by exploiting the spatial sparsity of harmonic sources, we extend the traditional observability analysis by showing that the underdetermined system can become observable under proper measurement arrangements. Then the estimation problem is formulated as a sparsity maximization problem which can be solved efficiently by linear programming.

The proposed algorithm is tested in a three-phase balanced IEEE 14-bus harmonic test system. Our results show that we can obtain reliable harmonic estimate for the underdetermined system with 13 unknown sources and only 9 meters when small measurement noises and model parameter deviations appear. In comparison, least-square based methods are unable to produce reliable estimates because they require the number of meters greater or equal to the total number of suspicious buses, which is 13 in this case.

By combining the new observability analysis and the sparsity maximization algorithm, the paper provides a strict approach for establishing a system-wide harmonic state estimator in large power systems at low cost. Such a harmonic state estimator can provide critical real-time information to correct harmonic related problems. The proposed method can also be applied to enhance the robustness of low-redundancy/ill-conditioned harmonic state estimation.

APPENDIX

The optimization problem (4) can be converted into a linear programming. Giving (4) as the following

$$\begin{array}{cc} \min_{\mathbf{x}} & \|\mathbf{x}\|_1 \\ \text{subject to} & \begin{cases} \|\mathbf{r}\|_1 \leq \varepsilon \\ \mathbf{z}-\mathbf{H}\mathbf{x} = \mathbf{r} \end{cases} \end{array} \tag{21}$$

By representing $\mathbf{x}$ and $\mathbf{r}$ by their positive and negative entries respectively

$$\begin{cases} \mathbf{x} = \mathbf{x}_u - \mathbf{x}_v \\ \mathbf{r} = \mathbf{r}_u - \mathbf{r}_v \\ \mathbf{x}_u, \mathbf{x}_v, \mathbf{r}_u, \mathbf{r}_v \geq \mathbf{0} \end{cases} \tag{22}$$

(21) takes the form

$$\begin{array}{ll} \min\limits_{\mathbf{x}_u,\mathbf{x}_v,\mathbf{r}_u,\mathbf{r}_v} & \sum_{k=1}^{n} (\mathbf{x}_u + \mathbf{x}_v) \\ \text{subject to} & \begin{cases} \sum_{k=1}^{n} (\mathbf{r}_u + \mathbf{r}_v) \leq \varepsilon \\ \mathbf{z} - \mathbf{H}(\mathbf{x}_u - \mathbf{x}_v) = \mathbf{r}_u - \mathbf{r}_v \\ \mathbf{x}_u, \mathbf{x}_v, \mathbf{r}_u, \mathbf{r}_v \geq \mathbf{0} \end{cases} \end{array} \tag{23}$$

Define a $(2n+2m)\times 1$ vector

$$\mathbf{y} = [\mathbf{x}_u^T, \mathbf{x}_v^T, \mathbf{r}_u^T, \mathbf{r}_v^T]^T \tag{24}$$

We obtain the equivalent linear programming

$$\begin{array}{ll} \min_{\mathbf{y}} & \mathbf{c}^T\mathbf{y} \\ \text{subject to} & \begin{cases} \mathbf{d}^T\mathbf{y} \leq \varepsilon \\ \mathbf{F}\mathbf{y} = \mathbf{z} \\ \mathbf{y} \geq \mathbf{0} \end{cases} \end{array} \tag{25}$$

where

$$\begin{cases} \mathbf{c} \triangleq [\mathbf{1}_{1\times n}, \mathbf{1}_{1\times n}, \mathbf{0}_{1\times m}, \mathbf{0}_{1\times m}]^T \\ \mathbf{d} \triangleq [\mathbf{0}_{1\times n}, \mathbf{0}_{1\times n}, \mathbf{1}_{1\times m}, \mathbf{1}_{1\times m}]^T \\ \mathbf{F} \triangleq \left[\begin{array}{cccc} \mathbf{H}_{m\times n} & -\mathbf{H}_{m\times n} & \mathbf{\Lambda}_{m\times m} & -\mathbf{\Lambda}_{m\times m} \end{array}\right] \end{cases} \tag{26}$$

where $\mathbf{1}$ is an all-one vector, $\mathbf{0}$ is an all-zero vector, $\mathbf{\Lambda}$ is an identity matrix.

ACKNOWLEDGMENT

The authors would like to thank Professor Marija Ilic in the Department of Electrical and Computer Engineering at Carnegie Mellon University for the initial discussion regarding this idea and the suggestions on revising the paper. I also wish to acknowledge the help received from Paul Hines, currently a PhD Candidate in the Department of Engineering and Public Policy and Carnegie Mellon Electricity Industry Center at Carnegie Mellon University, during revising the paper.

REFERENCES

[1] V. E. Wagner, J. C. Balda, D. C. Griffith, A. McEachern, T. M. Barnes, D. P. Hartmann, D. J. Phileggi, A. E. Emannuel, W. F. Horton, W. E. Reid, R. J. Ferraro, and W. T. Jewell, "Effects of harmonics on equipment," *IEEE Trans. Power Delivery* vol. 8, no. 2, pp. 672-680, 1993.

[2] *IEEE Recommended Practice and Requirements for Harmonic Control in Electrical Power System*, IEEE Standard 519-1992.

[3] G. T. Heydt, "Identification of harmonic sources by a state estimation technique," *IEEE Trans. Power Delivery,* vol. 4, no. 1, pp. 569-576, 1989.

[4] A. P. S. Meliopoulos, F. Zhang, and S. Zelingher, "Power system harmonic state estimation," *IEEE Trans. Power Delivery*, vol. 9, no. 3, pp. 1701-1709, 1994.

[5] Z. P. Du, J. Arrillaga, and N. Watson, "Continuous harmonic state estimation of power systems," *IEE Proc. Gener., Transm., & Distri.*, vol. 143, no. 4, pp. 329-336, 1996.

[6] Z. P. Du, J. Arrillaga, N. R. Watson, and S. Chen, "Identification of harmonic sources of power systems using state estimation," *IEE Proc. Gener., Transm., & Distri.*, vol. 146, no. 1,pp. 7-12, 1999.

[7] J. E. Farach, W. M. Grady, and A. Arapostathis, "An optimal procedure for placing sensors and estimating the locations of harmonic sources in power systems," *IEEE Trans. Power Delivery*, vol. 8, no. 3, pp. 1303-1310, 1993.

[8] N. R. Watson, J. Arrillaga, and Z. P. Du, "Modified symbolic observability for harmonic state estimation," *IEE Proc. Gener., Transm., & Distri.*, vol. 147, no. 2, pp. 105-111, 2000.

[9] A. Kumar, B. Das, and J. Sharma, "Genetic algorithm-based meter placement for static estimation of harmonic sources," *IEEE Trans. Power Delivery*, vol. 20, no. 2, pp. 1088-1096, 2005.

[10] C. Madtharad, S. Premrudeepreechacharn, N. R. Watson, and R. Saeng-Udom, "An optimal measurement placement method for power system harmonic state estimation," *IEEE Trans. Power Delivery*, vol. 20, no. 2, pp. 1514-1521, 2005.

[11] N. Kanao, M. Yamashita, H. Yanagida, M. Mizukami, Y. Hayashi, and J. Matsuki, "Power system harmonic analysis using state-estimation method for japanese field data," *IEEE Trans. Power Delivery*, vol. 20, no. 2, pp. 970-977, 2005.

[12] R. K. Hartana and G. G. Richards, "Harmonic source monitoring and identification using neural networks," *IEEE Trans Power Syst*., vol. 5, no. 4, pp. 1098-1104, 1990.

[13] H. M. Beides and G. T. Heydt, "Dynamic state estimation of power system harmonics using Kalman filter methodology," *IEEE Trans. Power Delivery,* vol. 6, no.4, pp. 1663-1670, 1991.

[14] H. Ma and A. A. Girgis, "Identification and tracking of harmonic sources in a power system using a Kalman filter," *IEEE Trans. Power Delivery,* vol. 11, no. 3, pp. 1659-1665, 1996.

[15] K. K. C. Yu, N. R. Watson, and J. Arrillaga, "An adaptive Kalman filter for dynamic harmonic state estimation and harmonic injection tracking," *IEEE Trans. Power Delivery,* vol. 20, no. 2, pp. 1577-1584, 2005.

[16] H. Liao and D. Niebur, "Load profile estimation in electric transmission networks using independent component analysis," *IEEE Trans. Power Syst.*, vol. 18, no. 2, pp. 707-715, 2003.

[17] D. Niebur, E. Gursoy, and H. Liao, "Independent component analysis techniques for power System load estimation - A signal-processing approach," in *Applied Mathematics For Restructured Electric Power-Optimization, Control, and Computational Intelligence*, J. C. Chow, F. F. Wu and J. A. Momoh, Ed. Springer Verlag, New York, NY 2004.

[18] H. Liao, "Power system harmonic state estimation via sparsity maximization," accepted by *Proc of IEEE/PES General Meeting 2006, Montréal, Canada*, June, 2006.

[19] R. Abu-Hashim, R. Burch, G. Chang, M. Grady, E. Gunther, M. Halpin, C. Hatziadoniu, Y. Liu, M. Marz, T. Ortmeyer, V. Rajagopalan, S. Ranade, P. Ribeiro, T. Sims, and W. Xu, "Test systems for harmonics modeling and simulation," *IEEE Trans. Power Delivery,* vol. 14, no. 2, pp. 579-587, 1999.

[20] D. L. Donoho and M. Elad, "Optimally sparse representation in general (nonorthogonal) dictionaries via L_1 minimization," *Proc. of Natl. Acad. Society*, vol. 100, pp. 2197-2202, 2003.

[21] A. Hyvarinen, J. Karhunen, and E. Oja, *Independent Component Analysis*, John Wiley & Sons, 2001.

[22] J. Nocedal and S. J. Wright, *Numerical Optimization*, Springer, 1999.

[23] J. Arrillaga, M. H. J. Bollen and N. R. Watson,"Power quality following deregulation," *Proceedings of the IEEE,* Vol. 88, no. 2, pp. 246-261. 2000.

Huaiwei Liao (M '2000) received his BS and MS from the Department of Electrical Engineering at Chongqing University in China. Currently, He is a Ph.D. candidate in the Department of Electrical and Computer Engineering at Carnegie Mellon University, Pittsburgh, PA. His interests include monitoring the risk of cascading failure, wide-area sensing and control, and power quality assessment in electric power systems.